



## Nanocalorimetric analysis of the ferromagnetic transition in ultrathin films of nickel

Aitor F. Lopeandía, F. Pi, and J. Rodríguez-Viejo

Citation: [Applied Physics Letters](#) **92**, 122503 (2008); doi: 10.1063/1.2901166

View online: <http://dx.doi.org/10.1063/1.2901166>

View Table of Contents: <http://scitation.aip.org/content/aip/journal/apl/92/12?ver=pdfcov>

Published by the [AIP Publishing](#)

---



## Re-register for Table of Content Alerts

Create a profile.



Sign up today!



# Nanocalorimetric analysis of the ferromagnetic transition in ultrathin films of nickel

Aitor F. Lopeandía, F. Pi, and J. Rodríguez-Viejo<sup>a)</sup>

Physics Department, Universitat Autònoma de Barcelona, 08193 Bellaterra, Spain

(Received 24 November 2007; accepted 4 March 2008; published online 25 March 2008)

We report on *in situ* heat capacity measurements (370–800 K) using quasiadiabatic ultrafast differential scanning nanocalorimetry in thin films (1–200 nm) of Ni grown by electron beam evaporation. The heat capacity shows a broad peak with a rounded maximum that is attributed to the decrease of long-range interactions in the ferromagnetic to paramagnetic phase transition of Ni. The calorimetric data exhibit a reduction of the Curie temperature as the thickness of the films (or the average grain size) decreases. The magnitude of the jump in specific heat at  $T_C$  scales with the number of surface or interface atoms. © 2008 American Institute of Physics.

[DOI: 10.1063/1.2901166]

Second-order or continuous phase transitions show a discontinuity in the second-order derivative of the Gibbs free energy with respect to temperature and pressure. Therefore, in a bulk solid, the measurement of the specific heat is a powerful tool to investigate phase transitions because it exhibits large variation near critical points. The theory of critical phenomena predicts a power law temperature dependence near the transition points.<sup>1</sup> In confined systems, the pioneering theoretical work of Fisher and Barber<sup>2</sup> showed that the Curie temperature  $T_C$  shifts to a lower temperature when the spin-spin correlation exceeds the film thickness. The dependence of  $T_C$  with dimensionality has been measured in ultrathin films of Ni (Refs. 3–5) and in other low-dimensional structures such as nanorods<sup>6</sup> and nanoparticles.<sup>7,8</sup> The dimensionality has an important effect on the shape and temperature of the magnetic transition<sup>9</sup> and the temperature dependence for the bulk material has been shown to be inappropriate for nanoparticles and nanowires.<sup>6,10</sup> Calorimetry, either in ac or scanning mode, has primarily been used on bulk samples because the amount of energy released by a phase transition in thin films or isolated nanoparticles is too small to be measured and analyzed with accuracy. A significant effort in recent years has been devoted to building sensitive membrane-based calorimeters to measure heat capacity in minute samples. These microsystems have already been demonstrated to work below 800 K as quasiadiabatic systems,<sup>11,12</sup> using ultrafast heating rates ( $10^4$ – $10^6$  K/s), or ac nanocalorimeters<sup>13</sup> with a very high sensitivity.

In this letter we report on the performance of membrane-based scanning nanocalorimetry in the analysis of lambda-type phase transitions in nanoscale thin films of Ni. We show that both the Curie temperature and the spike in specific heat at the transition are modified at smaller thicknesses. We also observe an increase in the specific heat with decreasing grain size.

A pair of identical nanocalorimeters with alumina-capped serpentine-type heaters are mounted inside a UHV e-beam chamber as previously described.<sup>14,15</sup> The nanocalorimeters are isothermally annealed at temperatures over 800 K to clean the silicon nitride membrane. Nevertheless, to prevent any undesired surface contamination, we grow a

10 nm SiO<sub>2</sub> buffer layer on both calorimetric cells at room temperature using a shadow mask. The film is e-beam evaporated from pure SiO<sub>2</sub> pellets under an oxygen rich atmosphere at  $10^{-3}$  mbar. Afterwards, the pressure is reduced again to  $10^{-7}$  mbar.

Hundreds of quasiadiabatic scans up to temperatures around 800 K were carried out in order to obtain an initial characterization of the calorimetric cells and the initial discrepancy in heat capacity between them (baseline correction). In order to apply power loss corrections which are needed for the quantitative measurement of specific heat, the calorimetric scans were performed at different heating rates by injecting pulses with different current values (15, 25, 40, and 50 mA). Subsequently, with the aid of a moving shutter, the Ni sample was selectively grown in one of the nanocalorimeters. The other calorimeter was used as a reference. Ni was evaporated from pure pellets in a high vacuum environment and the substrate was maintained at room temperature. The deposition rate was fixed at 0.25 nm/s by using a previously calibrated quartz crystal microbalance. Up to nine nominal thicknesses of Ni spanning 1–200 nm were grown and analyzed *in situ* by nanocalorimetry. In parallel, a set of moving shutters was used to deposit identical Ni thicknesses in the sub-10-nm range and the SiO<sub>2</sub> buffer layer onto 30 nm silicon nitride membranes used as grids for transmission electron microscopy (TEM) analysis.

The growth of Ni onto the SiO<sub>2</sub> layer occurs through a three-dimensional mechanism. At nominal thicknesses below 10 nm, the film is composed of nanometer size grains, as shown in Fig. 1. An islandlike morphology is clearly identified by TEM in the thinnest samples. Darker points in the TEM images (Fig. 1) correspond to thicker grains. For films thicker than 10 nm, the film is considered to be continuous and the average grain size in the perpendicular orientation roughly matches the film thickness, as confirmed by x-ray diffraction.

The heat capacity of the Ni thin films is determined from the raw data after applying the various correction steps discussed in Refs. 16 and 17. As an important step in this procedure, we apply heat loss corrections by using five different heating rates from  $2 \times 10^4$  to  $6 \times 10^4$  K/s for each thickness. Figure 2 shows in a semilogarithmic plot the heat capacity versus temperature for several Ni thicknesses evaluated at a

<sup>a)</sup>Electronic mail: javirod@vega.uab.es.

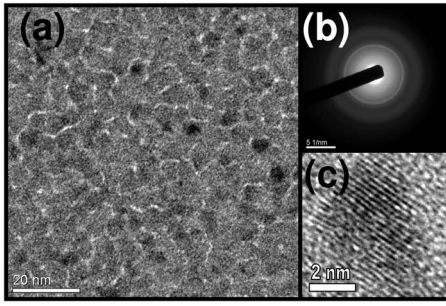


FIG. 1. (a) Planar view TEM picture of the 3 nm Ni film. (b) Electron diffraction pattern. (c) Detail of a nanosize grain.

heating rate of  $4.2 \times 10^4$  K/s. The heat capacity curves show a rounded peak at a temperature close to the Curie temperature of Ni. The continuous increase of heat capacity after the magnetic transition is due to the lattice contribution. The rounded appearance of the maximum in  $C_p$  is a characteristic feature of the measurements in this study and is likely related to the small size of the grains. The thinner films show a larger rounding effect, which is attributed to the reduction of the length scale of the magnetic interactions as the grain size decreases. Figure 3(a) shows the normalized Curie temperature measured in the calorimetric scan as a function of the average grain size for each film. The temperature of the transition is taken as the maximum in the heat capacity data. The smallest sizes are subject to considerable uncertainty due to the smooth shape of the  $C_p$  data at the transition temperature. However, there is a clear indication that  $T_C$  decreases as nanoparticle size decreases. Compared to the strong decrease of  $T_C$  in nanowires<sup>5</sup> or isolated nanoparticles,<sup>7</sup> our results are more consistent with a one-dimensional confinement, as is typically found in thin films.<sup>3-5</sup> As rounding poses a severe constraint on the analysis of the asymptotic behavior by a power law, we use the size-dependence model of the transi-

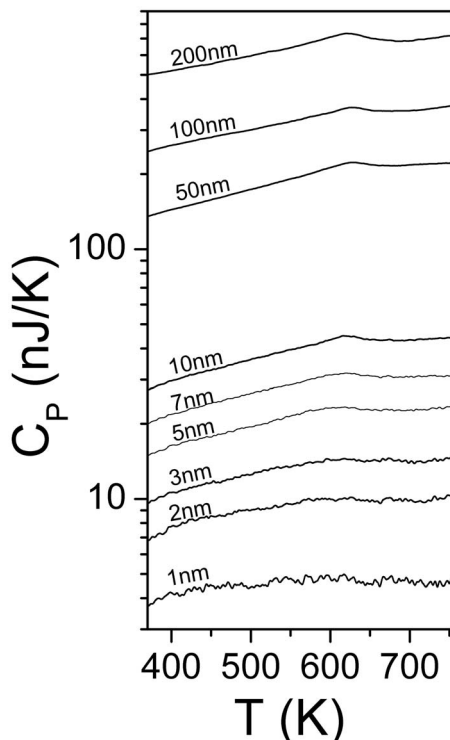


FIG. 2. Heat capacity vs temperature for Ni films of several thicknesses.

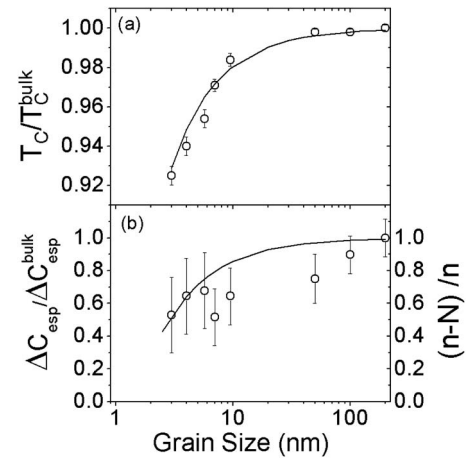


FIG. 3. (a) Relative Curie temperature as a function of the average particle diameter. The continuous line is derived from the model of Cui *et al.* (Ref. 18). (b) Relative variation of the specific heat jump at the Curie transition temperature as a function of film thickness. The continuous line represents the ratio of volume-to-surface atoms in disk-shaped nanograins.

tion developed by Cui *et al.*<sup>18</sup> to fit the experimental data. This model is based on thermodynamics and similarity arguments with other phase transitions, such as the glass transition. It predicts an exponential dependence of the Curie temperature with the well-defined bulk parameters

$$\frac{T_c}{T_{c0}} = \exp \left\{ - \frac{2\Delta C_{\text{esp}}}{3R[(D/D_0) - 1]} \right\}, \quad (1)$$

where  $\Delta C_{\text{esp}}$  denotes the specific heat difference between the bulk ferromagnetic phase and bulk paramagnetic phase at the bulk transition temperature,  $D$  is the nanoparticle diameter and  $2D_0$  represents the critical size where the Curie transition is still present. According to Cui *et al.*,<sup>18</sup> when the film thickness is below  $30h$  ( $h$ =interlayer distance, 2.492 Å in Ni), the film is considered to be discontinuous with an islandlike configuration, and the magnetic domains also show an islandlike pattern. The continuous line in Fig. 3(a) was obtained using standard bulk values and a fitting parameter  $D_0$  of 0.46 nm. The fitting parameter is strikingly similar to the value obtained from epitaxial Ni films grown on top of a Cu substrate (0.458 nm).<sup>3</sup> Figure 3(b) shows the jump in specific heat at the Curie temperature. The mass equivalent for every thickness is evaluated using the data of the 200 nm film as reference. Assuming that no size effects occur at this thickness, the mass is simply estimated by using the relation  $m = C_p / C_{\text{esp}}$ , using the tabulated value of  $C_{\text{esp}}$  at 350 K. This provides the relation between thickness and mass that we apply to all thicknesses in the series. The values of the thicker films agree with bulk literature values. The graph shows a reduction of the specific heat difference at  $T_C$  with decreasing grain size. Interestingly, the specific heat reduction scales with the number of volume to surface atoms,  $(n-N)/n$ , as shown by the continuous line of Fig. 3(b). This line is the relation between the number of surface atoms  $N$  and the total number of atoms  $n$  for a disk-shaped nanograin. In the molecular field approximation, the specific heat is proportional to the first derivative with temperature of the saturation magnetization or the magnetic moment. Therefore, the present data are consistent with a reduction of the magnetic moments of the surface or interface atoms. This occurs because spins at the surface have fewer spin interactions than

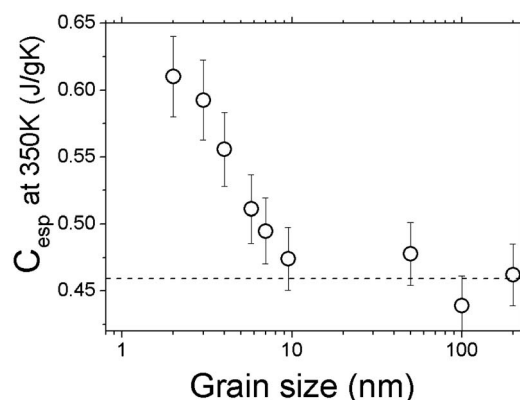


FIG. 4. Specific heat variation as a function of thickness evaluated at 350 K. The dashed line corresponds to the bulk value 0.459 J/g K.

those in the interior and the number of nearest magnetic interaction neighbors decreases.<sup>5</sup> This is also in agreement with previous studies of Ni clusters, 3 nm in diameter, showing that the average value of the saturation magnetization was  $0.4\mu_B/\text{atom}$ , significantly lower than the bulk value of  $0.6\mu_B/\text{atom}$ .<sup>19</sup> In addition, in Fig. 4, we plot the specific heat at 350 K as a function of the average grain size in the films. It is clearly observed that the nanocrystalline material exhibits enhanced specific heat compared to the bulk material. This is in agreement with past studies on Cu and Pd nanocrystalline materials.<sup>20</sup> As 350 K is well below the magnetic transition, we suggest that the rise in specific heat is mainly related to lattice vibrations and may be caused by the softening of surface phonons or by the contribution of grain boundaries.

In conclusion, we have shown that ultrafast differential scanning nanocalorimetry is a powerful tool to measure continuous phase transitions *in situ* at the nanoscale, including the ferromagnetic transition in Ni thin films. We have observed a decrease of the Curie temperature and of the specific heat difference between the ferromagnetic and paramagnetic

states as the average grain size decreases. We have also demonstrated the increase of specific heat as the film thickness (and grain size) decreases.

We thank O. Bourgeois and J. L. Garden for useful comments. This work was supported by Contract Nos. MAT2004-04761 and MAT2007-61521 granted by the Spanish Ministry of Education and Contract No. 2005SGR00201 granted by the Direcció General de Recerca of the Generalitat of Catalonia.

<sup>1</sup>D. L. Connelly, J. S. Loomis, and D. E. Mapother, *Phys. Rev. B* **3**, 924 (1971).

<sup>2</sup>M. E. Fisher and M. N. Barber, *Phys. Rev. Lett.* **28**, 1516 (1972).

<sup>3</sup>R. Zhang and R. F. Willis, *Phys. Rev. Lett.* **86**, 2665 (2001).

<sup>4</sup>Y. Li and K. Barbeschke, *Phys. Rev. Lett.* **68**, 1208 (1992).

<sup>5</sup>W. H. Zhong, C. Q. Sun, B. K. Tay, S. Li, H. L. Bai, and E. Y. Jiang, *J. Phys.: Condens. Matter* **14**, L399 (2002).

<sup>6</sup>L. Sun, P. C. Searson, and C. L. Chien, *Phys. Rev. B* **61**, R6463 (2000).

<sup>7</sup>D. Gerion, A. Hirt, I. M. Billas, A. Châtelain, and W. A. deHeer, *Phys. Rev. B* **62**, 7491 (2000).

<sup>8</sup>H. Amekura, Y. Fudamoto, Y. Takeda, and N. Kishimoto, *Phys. Rev. B* **71**, 172404 (2005).

<sup>9</sup>E. N. Abarra, K. Takano, F. Hellman, and A. E. Berkowitz, *Phys. Rev. Lett.* **77**, 3451 (1996).

<sup>10</sup>W. H. Zhong, C. Q. Sun, and S. Li, *Solid State Commun.* **130**, 602 (2004).

<sup>11</sup>S. L. Lai, G. Ramanath, L. H. Allen, P. Infante, and Z. Ma, *Appl. Phys. Lett.* **67**, 1229 (1995).

<sup>12</sup>M. Yu. Efremov, F. Schiettekatte, M. Zhang, E. A. Olson, A. T. Kwan, R. S. Berry, and L. H. Allen, *Phys. Rev. Lett.* **85**, 3560 (2000).

<sup>13</sup>O. Bourgeois, S. E. Skipetrov, F. Ong, and J. Chaussy, *Phys. Rev. Lett.* **94**, 057007 (2005).

<sup>14</sup>A. F. Lopeandía and J. Rodríguez-Viejo, *Thermochim. Acta* **461**, 82 (2007).

<sup>15</sup>A. F. Lopeandía, J. Rodríguez-Viejo, M. Chacón, M. T. Clavaguera-Mora, and F. J. Muñoz, *J. Micromech. Microeng.* **16**, 965 (2006).

<sup>16</sup>M. Yu. Efremov, E. A. Olson, M. Zhang, S. L. Lai, F. Schiettekatte, Z. S. Zhang, and L. H. Allen, *Thermochim. Acta* **412**, 13 (2004).

<sup>17</sup>A. F. Lopeandía, Ph.D. thesis, Universitat Autònoma de Barcelona, 2007.

<sup>18</sup>X. F. Cui, M. Zhao, and Q. Jiang, *Thin Solid Films* **472**, 328 (2005).

<sup>19</sup>Y. Volokitin, J. Sinzig, G. Schmid, H. Bönneman, and L. J. DeJongh, *Z. Phys. D: At., Mol. Clusters* **40**, 136 (1997).

<sup>20</sup>J. Rupp and R. Birringer, *Phys. Rev. B* **36**, 7888 (1987).